Received: 7 September 2023 | Revised: 2 February 2024 | Accepted: 9 February 2024

DOI: 10.1002/jez.2799

RESEARCH ARTICLE

JEZ-A ECOLOGICAL AND INTEGRATIVE PHYSIOLOGY WILEY

Ultrasound images of the ascending aorta of anesthetized northern fur seals and Steller sea lions confirm that the aortic bulb maintains continuous blood flow

Rhea L. Storlund[1,2] | David A. S. Rosen[1,3] | Martin Haulena[3] | Shubhayan Sanatani[4,5] | Jessica Vander Zaag[4] | Andrew W. Trites[1,2]

[1]Marine Mammal Research Unit, Institute for the Oceans and Fisheries, University of British Columbia, Vancouver, British Columbia, Canada

[2]Department of Zoology, University of British Columbia, Vancouver, British Columbia, Canada

[3]Vancouver Aquarium, Vancouver, British Columbia, Canada

[4]Division of Cardiology, British Columbia Children's Hospital, Vancouver, British Columbia, Canada

[5]Department of Pediatrics, University of British Columbia, Vancouver, British Columbia, Canada

Correspondence
Rhea L. Storlund
Email: r.storlund@oceans.ubc.ca

Funding information
Natural Sciences and Engineering Research Council of Canada; ReNewZoo

Abstract

The increased size and enhanced compliance of the aortic bulb—the enlargement of the ascending aorta—are believed to maintain blood flow in pinnipeds during extended periods of diastole induced by diving bradycardia. The aortic bulb has been described ex vivo in several species of pinnipeds, but in vivo measurements are needed to investigate the relationship between structure and function. We obtained ultrasound images using electrocardiogram-gated transesophageal echocardiography during anesthesia and after atropine administration to assess the relationship between aortic bulb anatomy and cardiac function (heart rate, stroke volume, cardiac output) in northern fur seals (*Callorhinus ursinus*) and Steller sea lions (*Eumetopias jubatus*). We observed that the aortic bulb in northern fur seals and Steller sea lions expands during systole and recoils over the entire diastolic period indicating that blood flow is maintained throughout the entire cardiac cycle as expected. The stroke volumes we measured in the fur seals and sea lions fit the values predicted based on body size in mammals and did not change with increased heart rates, suggesting that greater stroke volumes are not needed for aortic bulb function. Overall, our results suggest that peripheral vasoconstriction during diving is sufficient to modulate the volume of blood in the aortic bulb to ensure that flow lasts over the entire diastolic period. These results indicate that the shift of blood into the aortic bulb of pinnipeds is a fundamental mechanism caused by vasoconstriction while diving, highlighting the importance of this unique anatomical adaptation.

KEYWORDS
aortic bulb, atropine, cardiovascular, heart rate, pinniped, stroke volume, transesophageal echocardiography

1 | INTRODUCTION

The circulatory systems of marine mammals evolved to support breath-hold diving (herein diving) (reviewed in Ponganis, 2015) which is critical for both foraging and predator avoidance. Diving is physiologically challenging because marine mammals depend on limited oxygen stores to fuel their activity underwater which cannot be replenished until they surface to breathe. Marine mammals prolong their dives by carrying increased oxygen stores in their bodies (i.e., increased supply) and evoking physiological responses to conserve oxygen (i.e., reduced demand) (reviewed in Kooyman & Ponganis, 1998). Cardiovascular adaptations that increase oxygen storage capacity include large blood volumes, high hematocrit (concentrations of red blood cells), venous and splenic reserves of oxygenated blood—while vasoconstriction is the main physiological adaptation to conserve oxygen (Blix, 2018; Butler, 1982; Cabanac, 2000, 2002; Castellini et al., 2010; Kooyman & Ponganis, 1998; Qvist et al., 1986; Stephenson, 2005).

By constricting peripheral blood vessels, marine mammals can direct blood flow toward the brain and other oxygen-sensitive tissues—and away from tissues that do not require oxygenated blood during diving (e.g., muscles which can rely on myoglobin-bound oxygen, or less active tissues) (Elsner et al., 1966; Zapol et al., 1979). On its own, vasoconstriction would detrimentally increase mean arterial blood pressure if it were not counteracted by a concomitant decrease in heart rate (HR) (diving bradycardia) (Butler, 1982). However, slowed HRs leave a longer pause between cardiac contractions which must be bridged by the vasculature to maintain continuous blood flow.

Among mammals, the ascending aorta (Asc Ao) contributes to blood flow maintenance during diastole. The Asc Ao is a compliant vessel that expands to accommodate the blood pumped out of the left ventricle during systole, and then elastically recoils, releasing a steady flow of blood when the left ventricle relaxes during diastole (Nichols et al., 2011). This smooths the otherwise pulsatile pressure wave that the heart would generate as it discontinuously pumps blood to the body. This function is especially important in species that regularly attain low HRs, such as diving marine mammals, because of the long diastolic pause between heartbeats (Blix et al., 1984; King, 1977; Rhode et al., 1986).

The specific adaptation of the aorta to support the cardiovascular changes during diving differs among marine mammals. In pinnipeds, the diameter of the Asc Ao increases after it leaves the heart and forms a bulbous structure referred to as the aortic bulb (AB) (Figure 1) (Blix et al., 2016; Dennison et al., 2009; Drabek, 1975; Elsner et al., 1966; Guimarães et al., 2014; King, 1977; Murie, 1874; Nie, 1985; Rhode et al., 1986). In fin whales, there is no noticeable bulbous enlargement; instead, the aortic arch is larger and more compliant than the descending aorta (Shadwick & Gosline, 1994). In both pinnipeds and fin whales the enlargement or enhanced compliance has the potential to accommodate a greater volume of blood than could a smaller or stiffer blood vessel.

In theory, the energy stored in the elastic recoil of the aorta is used to maintain continuous blood flow for longer interbeat durations required during bradycardia in diving mammals. Perhaps most importantly, based on anatomical observations, the enhanced size and compliance of marine mammal aortas has been hypothesized to contribute to maintaining blood flow to the brain while attaining extremely low HRs (Blix et al., 2016; Drabek, 1975; Elsner et al., 1966; Nie, 1985; Shadwick & Gosline, 1995). To date, continuous blood flow during bradycardia has only been confirmed in one species (juvenile elephant seals, *Mirounga angustirostris*) during forced dives in an magnetic resonance imager (Thornton et al., 2005).

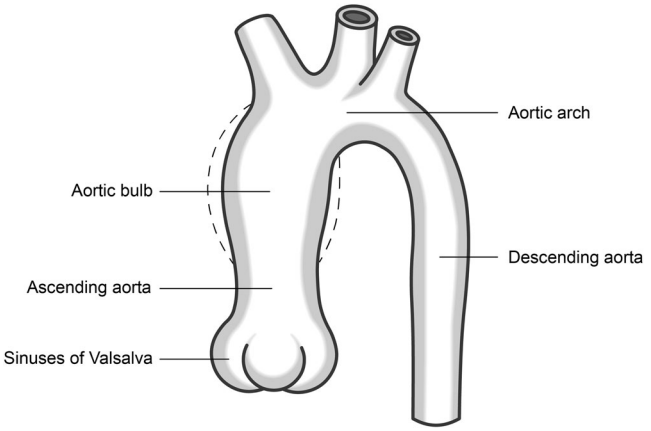

FIGURE 1 Diagram of a pinniped aorta showing the aortic bulb. Dashed lines represent the expansion of the aortic bulb that occurs when aortic pressure increases (e.g., during systole). When aortic pressure decreases (e.g., during diastole), the aortic bulb returns to its less pressurized state. Illustration by Anderson Li.

Another hypothesized benefit of greater aortic compliance is the ability to decrease myocardial work (Campbell et al., 1981; Ponganis, 2015; Rhode et al., 1986). With each contraction, the left ventricle must generate enough force to overcome the pressure in the Asc Ao (cardiac afterload) to open the aortic valve and eject blood. However, constricting peripheral blood vessels during diving runs the risk of increasing cardiac afterload, which can be mediated by the left ventricle pushing against the compliant walls of the aorta instead of pushing against the high pressure generated by peripheral resistance. The more compliant the aortic walls are, the less work the left ventricle needs to expend to eject blood, thereby conserving oxygen with each heartbeat (Campbell et al., 1981).

While it has been assumed that the aortas of marine mammals are to support diving, functional assessments of the AB are lacking because in vivo measurement techniques have been challenging to perform on marine mammals. We chose to use transesophageal echocardiography to evaluate the size and function of the aorta in anesthetized Steller sea lions and northern fur seals. Transesophageal echocardiography places the ultrasound probe directly behind the heart and aortic arch, overcoming the technical shortfalls associated with transthoracic echocardiography in marine mammals. Studying live animals provided the opportunity to evaluate dynamic changes in aortic dimensions within the cardiac cycle and at different HRs. It also allowed us to make in vivo anatomical and functional measurements

that cannot be obtained ex vivo. Specifically, we compared the aortas of northern fur seals (*Callorhinus ursinus*) and Steller sea lions (*Eumetopias jubatus*) (two closely related, but size dimorphic otariid species) by taking anatomical measurements of the Asc Ao, calculating stroke volume (SV), and recording changes in AB size with HR and the cardiac cycle.

2 | METHODS

2.1 | Overview

Electrocardiogram (ECG)-gated transesophageal echocardiograms were performed on northern fur seals and Steller sea lions to describe the Asc Ao and assess AB function. The Asc Ao was examined twice during isoflurane anesthesia—before and after atropine administration—to investigate the effects of HR changes on AB function. All research was conducted under the approval of the Animal Care Committees at the Vancouver Aquarium and University of British Columbia (Permit A21-0034).

2.2 | Animals

Transesophageal echocardiograms were performed on five adult female fur seals (13–14 years; 27.2–43.5 kg), six adult female sea lions (16–24 years; 180.0–225.6 kg), and one 4-year-old female sea lion (139.0 kg) cared for at the Vancouver Aquarium. All animals were healthy and not pregnant at the time of the procedure.

2.3 | Anesthesia

All animals were masked and anesthetized with 1%–5% isoflurane in oxygen under the supervision of a veterinarian (M. H.) following previously described protocols (Haulena, 2014; Storlund et al., 2021). Once an adequate plane of anesthesia was reached, individuals were intubated with an appropriately sized endotracheal tube (fur seals: 7–9 mm; sea lions: 16–18 mm). Mechanical and manual ventilation were used to supplement spontaneous breathing as needed. Three fur seals (NFS08AN, NFS08ME, NFS08TI) were mechanically ventilated using a Hallowell model 2002 ventilator and four Steller sea lions (F00AS, F17BE, F97HA, F97SI) were mechanically ventilated using a SurgiVet large animal anesthetic machine. Ventilator settings were 15–20 mL/kg tidal volume and six breaths per minute. HR, breathing frequency, rectal temperature, and SPO_2 were monitored throughout the procedure. Mean ± SD spontaneous breathing frequencies were 9 ± 4 breaths per minute, rectal temperatures were 34.2 ± 0.6°C, and SPO_2 was 96 ± 4% in both the fur seals and sea lions, and there were no noticeable changes in these parameters after atropine administration. Three sea lions (F17BE, F03IZ, F03RO) received 0.15 mg/kg diazepam orally 50–70 min before anesthesia. Total anesthetic duration ranged from 45 to 79 min and animals recovered in 10–20 min.

2.4 | Transesophageal echocardiogram procedure

ECG-gated transesophageal echocardiograms were performed by a cardiologist (S. S.) and cardiac sonographer (J. V. Z.) using a GE LOGIQ e ultrasound with a 6Tc-RS transesophageal echocardiography probe and ECG module. Animals were positioned in sternal recumbency, and three ECG leads were attached: two in the axillary region of the fore flippers and the third on the insertion of the hind flipper. The electrodes and surrounding area were wetted with 70% isopropyl alcohol to enhance conductivity. Slight adjustments to electrode positioning or supplemental wetting with 70% isopropyl alcohol were made as needed to maintain the clarity of the ECG signal. Optimal probe positioning was determined by the cardiologist and images and recordings were captured by the cardiac sonographer for subsequent measurements. For consistency, all measurements were made by one cardiac sonographer except for the dynamics measurements which were made by another researcher (R. L. S.; see Section 2.7).

2.5 | Views and measurements

We obtained midesophageal aortic valve long axis (probe angle range: 65–128°) and midesophageal ascending aortic long-axis views (probe angle range: 77–124°) (Figure 2). Images of the left ventricular outflow tract (LVOT), sinuses of Valsalva (SoV), sinotubular junction (STJ), proximal tubular portion of the Asc Ao, AB, and aortic intima-media thickness (Ao IMT) were obtained using B-mode. The maximum velocity of the LVOT flow profile (LVOT V_{max}) and LVOT velocity–time integral (LVOT VTI) were measured using Doppler. Left ventricular SV was calculated from the LVOT VTI and LVOT using the formula: Stroke volume = $\pi \times \left(\frac{\text{LVOT}}{2}\right)^2 \times \text{VTI}$. Cardiac output (CO) was calculated as the product of SV and HR. Images of the left ventricle could not be reliably obtained using transesophageal echocardiography and are not presented in this study.

One to six repeat mid-systolic anatomical measurements were made for each individual animal using the inner-edge-to-inner-edge technique. First a single value (maximum or mean) was calculated for each animal, then a summary value was calculated for each species. For each animal, the maximum value was used for structures that were measured from longitudinal sections of the aorta (LVOT, SoV, STJ, Asc Ao, and AB). These structures can always be larger than the reported measurement due to how the cylindrical vessel is sectioned to produce the image. As a result, the largest value recorded is the most accurate, but may still represent an underestimate. For each animal, means were calculated for intima-media thickness, HR, LVOT V_{max}, LVOT VTI, left ventricular SV, and CO. Measurements are summarized for each species as medians (interquartile range [IQR]),

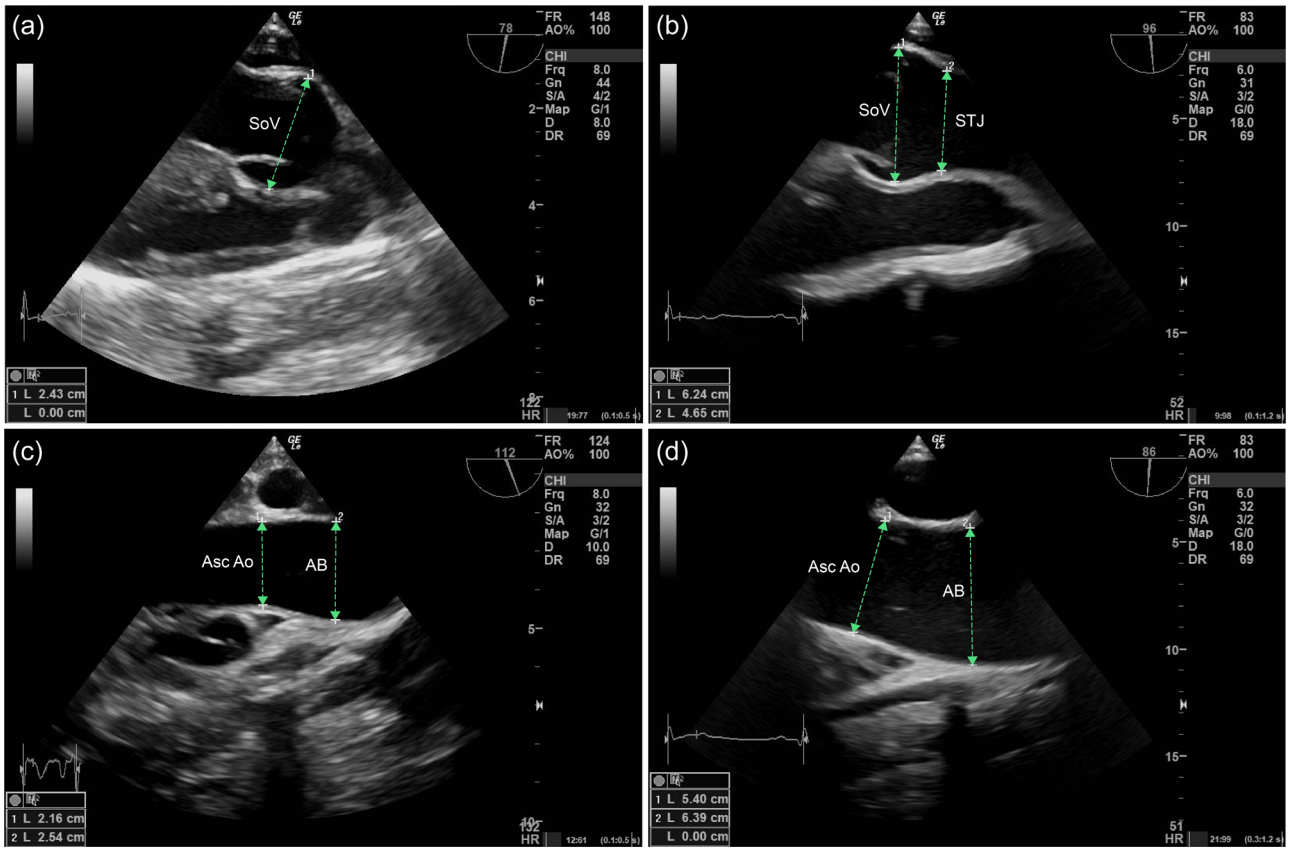

FIGURE 2 Midesophageal aortic valve long-axis view (a and b) and midesophageal ascending aortic long-axis view (c and d) of northern fur seals (left; a and c) and Steller sea lions (right; b and d). Sample measurements of the sinuses of Valsalva (SoV), sinotubular junction (STJ), ascending aorta (Asc Ao), and aortic bulb (AB) are shown with green arrows.

and values for the smaller 4-year-old sea lion are presented separately. Individual values are available in Supporting Information S1: Tables S1 and S2.

2.6 | Atropine

To evaluate the effect of HR on AB dimensions, a total dose of 0.015–0.035 mg/kg atropine was administered in up to three injections with the aim of increasing HR by 20%. Each animal received an initial dose of atropine (0.01–0.02 mg/kg) and if their HR did not increase sufficiently, additional atropine was administered at the veterinarian's discretion. Atropine was delivered via a butterfly catheter in an interdigital vessel in a hind flipper. Atropine was administered 31–64 min after initial masking depending on how quickly the initial transesophageal echocardiography measurements were obtained. One-to-two-beat video recordings of the AB in the midesophageal ascending aortic long-axis view were collected during anesthesia and after atropine administration to be measured offline. In four animals, HR did not increase appreciably, and the procedure was ended without collecting postatropine measurements.

2.7 | Dynamic AB measurements

To compare the size of the AB pre- and postatropine administration and during the cardiac cycle, videos of the AB were reviewed and selected for further analysis. Videos that included a minimum of one complete cardiac cycle (i.e., showed two clear ECG complexes) and displayed a reasonable instantaneous HR were included. For individuals that had more than one video that could be included for each treatment (pre- and postatropine), the video with better image quality was used. Similarly, for videos that captured multiple beats, the beat that had more of the AB visible or better image quality was used.

Videos were opened in Fiji (Schindelin et al., 2012) and frames showing mid-systole (onset of the T-wave) and end-diastole (onset of the QRS complex) were extracted for measurements. Because the aorta shifts positions during the cardiac cycle, measurements were standardized using an anatomical marker that was visible in both mid-systole and end-diastole. Two AB measurements were made on each frame. The first measurement was AB diameter standardized to a landmark on the posterior wall of the aorta. The second is a custom AB measurement that approximated changes in volume by incorporating changes in both diameter and length of the AB during the

cardiac cycle. Detailed measurement descriptions and images are provided in the supplementary materials.

2.8 | Statistical analysis

Statistical analyses were performed using R (R Core Team, 2022) and RStudio (RStudio Team, 2022). To evaluate the size of the AB in northern fur seals and Steller sea lions with respect to other mammals, we calculated the expected diameter of the Asc Ao based on body weight (BW) expressed in kg using the equation: $\text{AscAo} = 0.41 \times \text{BW}^{0.36}$ (Holt et al., 1981), and calculated how much larger the AB is than expected using the equation:

$$\text{Percent difference in AB diameter} = \frac{\text{AB diameter} - \text{Expected Asc Ao diameter}}{\left(\frac{\text{AB diameter} + \text{Expected Asc Ao diameter}}{2}\right)} \times 100\%.$$

To compare the HRs, SVs, and COs that we measured in anesthetized fur seals and sea lions with the values predicted from allometric scaling, we calculated expected values using the equations:

$$\text{Heartrate (bpm)} = 241 \cdot \text{BW}^{-0.25}$$

(Stahl, 1967),

$$\text{Heart rate (bpm)} = 191 \cdot \text{BW}^{-0.18}$$

(Mortola, 2015),

$$\text{Stroke volume (mL)} = \frac{\text{Cardiac output}}{\text{Heart rate}} = \frac{187 \times \text{BW}^{0.81}}{241 \times \text{BW}^{-0.25}} = 0.776 \cdot \text{BW}^{1.06}$$

(Stahl, 1967),

$$\text{Stroke volume (mL)} = \frac{\text{Cardiac output}}{\text{Heart rate}} = \frac{219 \times \text{BW}^{0.76}}{191 \times \text{BW}^{-0.18}} = 1.149 \cdot \text{BW}^{0.94}$$

(Mortola, 2015; Casha et al., 2017),

$$\text{Cardiac output (L/min)} = 0.187 \cdot \text{BW}^{0.81}$$

(Stahl, 1967), and

$$\text{Cardiac output (L/min)} = 0.219 \cdot \text{BW}^{0.76}$$

(Casha et al., 2017), where BW is expressed in kilograms. We calculated the equation for CO from Casha and colleagues (2017) by substituting the equation they provided relating heart mass and body mass ($\log \text{heartmass} = 1.0663 \cdot \log \text{BW} + 0.5955$) into the equation they provided relating CO and heart mass in similarly sized mammals ($\log \text{cardiacoutput} = 0.7127 \cdot \log \text{heartmass} + 1.9168$). Paired *t* tests were run to evaluate the effects of atropine on HR and SV after excluding outliers. Outliers (values above the third quartile + 1.5 times the IQR and below the first quartile−1.5 times the IQR) were identified using boxplot methods (rstatix package) (Kassambara, 2023). The normality of the difference in HR and SV pre- and postatropine was assessed using the Shapiro–Wilk normality test (rstatix package) (Kassambara, 2023). Two-way ANOVAs were run to test the effects of cardiac timing and HR on AB diameter and the custom AB measurement. The assumptions of ANOVA were assessed using Levene's test for homogeneity of variance across groups (car package) (Fox & Weisberg, 2019) and the Shapiro–Wilk normality test (rstatix package) (Kassambara, 2023).

3 | RESULTS

3.1 | Steller sea lion and northern fur seal aorta anatomy

Median (IQR) measurements of LVOT, SoV, STJ, Asc Ao, AB, and Ao IMT in the northern fur seals and Steller sea lions are presented in Table 1. Individual values for each parameter are available in Supporting Information S1: Table S1. Both the fur seals and sea lions have enlarged aortas consistent with previous descriptions of the pinniped AB. The diameter of the proximal Asc Ao increases from the LVOT to the SoV, then narrows for the tubular portion of the Asc Ao, and then increases again at the widest part of the AB (Figures 1 and 2; Table 1). The median (IQR) diameter of the widest part of the AB was 2.47 (2.22–2.74) cm in the northern fur seals and 5.76 (5.50–6.20) cm in the Steller sea lions (Table 1). In one fur seal and one sea lion, we viewed the aortic arch and proximal descending aorta and observed the expected narrowing of the aorta distal to the AB. In the northern fur seals, the proximal transverse arch measured 1.61 cm and was smaller than all other aortic diameter measurements including the LVOT (1.94 cm). In the Steller sea lions, the proximal transverse aortic arch measured 3.60 cm and was smaller than the SoV (4.51 cm) and AB (4.05 cm), but larger than all other ascending aortic diameter measurements. The intima-media thickness of the wall of the aorta was 0.14 (0.14–0.14) cm in the fur seals and 0.27 (0.25–0.29) cm in the sea lions. Measurements from a 4-year-old female sea lion are presented separately (Table 1) because this animal was much smaller than the adults (139.0 vs. 198.9 kg) and had smaller aortic diameters.

In all individuals, the diameter of the AB was approximately the same as the SoV. The AB:SoV was 1.01 (0.93–1.07) in the northern fur seals, 1.01 (0.97–1.04) in the Steller sea lions and 0.90 in the 4-year-old sea lion. AB diameter standardized to BW was 0.07 (0.07–0.08) cm/kg in the fur seals, 0.03 (0.03–0.03) cm/kg in the sea lions, and 0.03 cm/kg in the 4-year-old sea lion.

Median (IQR) measurements of HR, LVOT Vmax, LVOT VTI, LVSV, and LVCO are presented in Table 2. The northern fur seals had an SV smaller SV (33.5 [25.2–46.8] mL) and a higher HR (122.5 [119.2–127.2] bpm) than the Steller sea lions (163.6 [124.2–206.2] mL and 57.0 [56.0–58.0] bpm). LVCO was 4.35 (3.38–5.74) L/min in the fur seals and 8.56 (7.03–12.03) L/min in adult sea lions.

TABLE 1 Physical characteristics of the ascending aorta of adult female northern fur seals and Steller sea lions.

	Northern fur seals (13–14 years)			Steller sea lions (16–24 years)			Steller sea lion (4 years; $n = 1$)
	n	Median	IQR	*n*	Median	IQR	Value
Body weight (kg)	5	35.8	30.8–35.8	6	198.9	190.8–211.4	139.0
LVOT (cm)	5	1.90	1.89–1.92	6	3.68	3.56–3.86	3.28
SoV (cm)	5	2.47	2.45–2.48	6	5.95	5.56–6.18	4.51
STJ (cm)	4	2.08	2.00–2.17	6	4.80	4.47–5.09	3.42
Asc Ao (cm)	5	1.88	1.79–2.27	5	4.72	4.21–5.13	3.28
AB (cm)	5	2.47	2.22–2.74	6	5.76	5.50–6.20	4.05
Ao IMT (cm)	4	0.14	0.14–0.14	5	0.27	0.25–0.29	0.20

Note: All animals were anesthetized with isoflurane anesthesia.

Abbreviations: AB, aortic bulb; Ao IMT, aorta intima-media thickness; Asc Ao, ascending aorta; IQR, interquartile range; LVOT, left ventricular outflow tract; SoV, sinuses of Valsalva; STJ, sinotubular junction.

TABLE 2 Doppler echocardiography measurements of northern fur seals and Steller sea lions.

	Northern fur seals (13–14 years)			Steller sea lions (16–24 years)			Steller sea lion (4 years; $n = 1$)
	n	Median	IQR	*n*	Median	IQR	Value
Body weight (kg)	5	35.8	30.8–35.8	5	199.2	198.6–215.4	139.0
HR (bpm)	4	122.5	119.2–127.2	5	57.0	56.0–58.0	80.0
LVOT Vmax (m/s)	4	0.69	0.63–1.11	5	0.92	0.50–1.07	0.94
LVOT VTI (cm)	4	11.29	8.58–17.46	5	11.98	11.40–21.98	17.45
LVSV (mL)	4	33.5	25.2–46.8	5	163.6	124.2–206.2	131.0
LVCO (L/min)	4	4.35	3.38–5.74	5	8.56	7.03–12.03	10.43

Note: All animals were anesthetized with isoflurane anesthesia.

Abbreviations: HR, heart rate; LVCO, left ventricular cardiac output calculated from Doppler measurements; LVOT Vmax, left ventricular outflow tract maximum velocity; LVOT VTI, left ventricular outflow tract velocity–time integral; LVSV, left ventricular stroke volume calculated from Doppler measurements.

Values for the 4-year-old sea lion are presented separately in Table 2. Individual values for HR, SV, and CO with corresponding allometric predictions are available in Supporting Information S1: Table S2.

Both the northern fur seals and the Steller sea lions had larger Asc Aos than predicted based on a scaling equation calculated for terrestrial mammals (Holt et al., 1981) and the AB was even larger than the Asc Ao in both species (Figure 3). The AB of the sea lions was 72.8% (67.8%–75.2%) larger than expected and the AB of the fur seals was 58.9% (40.8%–57.9%) larger than expected.

Using the median body mass of each species, the predicted SV was 34.4 mL in the northern fur seals and 212.4 mL in the Steller sea lions using $SV = 0.776 \cdot BW^{1.06}$ (Stahl, 1967) and 33.2 mL for northern fur seals and 166.5 mL for Steller sea lions using $SV = 1.149 \cdot BW^{0.94}$ (Casha et al., 2017; Mortola, 2015). For the fur seals, the predicted values are very similar to the value we measured from the anesthetized fur seals of 33.5 mL. For the sea lions, one of the predicted SVs is higher than we measured from the anesthetized sea lions of 163.6 mL, but less than the highest average value we calculated of 252.2 mL from the sea lion weighing 198.6 kg, while the second predicted SV is quite similar to what we measured. Using the body mass of each individual (rather than median mass) also demonstrates that the SVs we measured are similar to predicted values (Supporting Information S1: Table S2).

3.2 | Effects of atropine on HR and SV in anesthetized steller sea lions and northern fur seals

3.2.1 | Effects of atropine on HR

Overall, atropine had a statistically significant effect on the HRs of the Steller sea lions but not the northern fur seals. The HRs of the adult sea lions ($n = 5$) increased by 26.5 ± 13.1% (mean ± SD), from 53.8 to 67.8 bpm after atropine administration ($t = -4.81$, $df = 4$, $p = 0.009$). In contrast, the HR of the 4-year-old sea lion decreased

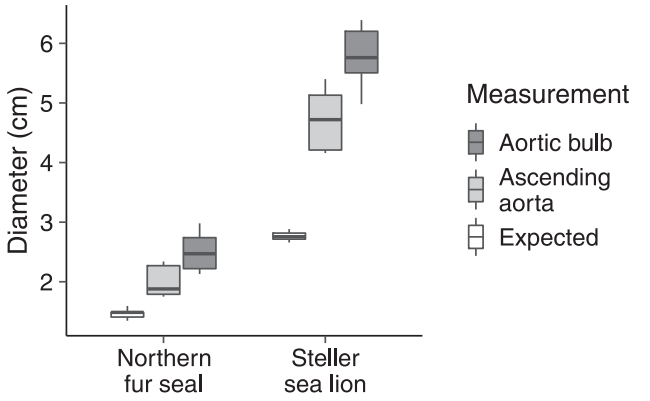

FIGURE 3 The diameter of the aortic bulb (dark gray), ascending aorta (light gray) of Steller sea lions ($n = 5$) and northern fur seals ($n = 5$) was greater than expected (white) according to a scaling equation calculated for terrestrial mammals (ascending aorta diameter = 0.41(body weight)$^{0.36}$, (Holt et al., 1981)). Within each box, horizontal black lines denote median values, boxes extend from the 25th to 75th percentile, whiskers denote adjacent values (i.e., the maximum and minimum values within 1.5 times the interquartile range).

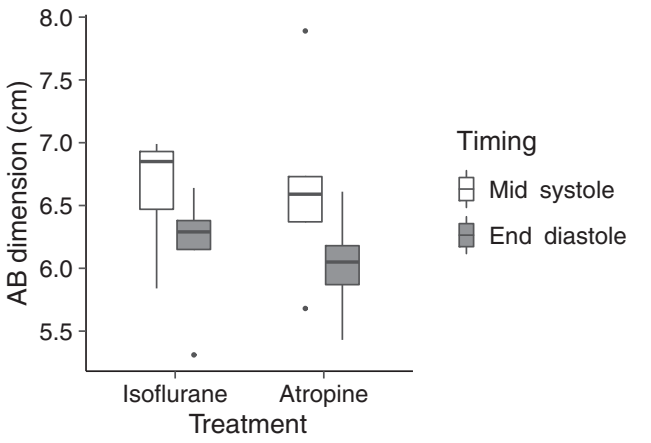

FIGURE 4 Cardiac timing influences aortic bulb dimension ($F_{(1,17)} = 1.47$, $p = 0.04$), but treatment does not ($F_{(1,17)} = 0.01$, $p > 0.8$). Within each box, horizontal black lines denote median values, boxes extend from the 25th to 75th percentile, whiskers denote adjacent values (i.e., the maximum and minimum values within 1.5 times the interquartile range), and dots denote data points that fall outside 1.5 times the interquartile range.

8% from 75.0 to 69.0 bpm after receiving atropine; this difference was identified as an outlier and was excluded from the pre- versus postatropine HR comparison. The change in HR after atropine administration was not consistent among the northern fur seals; HR increased in four fur seals and decreased in one fur seal. In one fur seal, HR increased 21.4% from 106.0 to 128.7 bpm after receiving atropine, but this difference was an outlier and was excluded from further analysis. Among the other fur seals ($n = 4$) HRs were not significantly different after atropine administration ($t = -1.49$, $df = 3$, $p > 0.2$).

3.2.2 | Effects of atropine on SV

Overall, atropine did not have a statistically significant effect on SV. Steller sea lion ($n = 4$) SVs increased 18.7 ± 12.0% (mean ± SD) from 186.5 to 218.4 mL after atropine administration, but this increase was not statistically significant ($t = -2.86$, $df = 3$, $p = 0.06$). We were unable to obtain VTIs in one of the treatments for three out of five northern fur seals and, therefore, could not calculate LVSV for these individuals. In the remaining two fur seals, SVs decreased by 18.1% from 22.7 to 18.6 mL and 41.17% from 64.4 to 37.9 mL after atropine administration, but the statistical significance of this effect could not be assessed due to small sample size.

3.3 | AB dynamics in Steller sea lions

Measurements of the AB at mid-systole and end-diastole from one- or two-beat video recordings of the proximal Asc Ao and AB in the Steller sea lions showed that the AB dimension was greatest during mid-systole ($F_{(1,17)} = 1.47$, $p = 0.04$), and that there was no effect of atropine on the change in AB dimension ($F_{(1,17)} = 0.01$, $p > 0.9$; Figure 4). AB dimensions decreased 8.73 (4.95–9.08)% from mid-systole to end-diastole during isoflurane and 7.85% (6.22%–10.10%) postatropine ($F_{(1,17)} = 1.47$, $p = 0.04$). In contrast, AB diameter, which is accounted for in the AB dimension measurement, was not affected by cardiac timing ($F_{(1,17)} = 1.31$, $p > 0.3$) or atropine ($F_{(1,17)} = 0.18$, $p > 0.68$).

4 | DISCUSSION

Our goal was to understand how the AB functions in pinnipeds by examining its anatomy, its movement during the cardiac cycle, and its relationship to cardiac function in northern fur seals and Steller sea lions. Although not all cardiac function measurements could be obtained (e.g., blood pressure), our study provides the most complete in vivo assessment of the AB in pinnipeds and includes measurements of HR, SV, and CO. Our direct measurements in northern fur seals and Steller sea lions provide an anatomical description of the AB and show how it responds to changes in blood flow during the cardiac cycle. Although our in vivo measurements are tempered by the known effects of anesthesia on HRs, SVs, and vasodilation in mammals, they are consistent with physiological expectations. Thus, they permit exploring connections between the AB, HR, and SV, and species-specific responses to atropine.

4.1 | Northern fur seal and Steller sea lion aorta anatomy

The Asc Aos of northern fur seals and Steller sea lions matched the general description of aortas of pinnipeds (e.g., Drabek, 1975;

Murie, 1874). Most notably, the Asc Ao widened from the LVOT to the SoV, narrowed for a short tubular portion, widened again as the AB, then narrowed as the proximal transverse arch and continued tapering as the descending aorta (Figure 1). This differs from the typical mammalian Asc Ao, which is widest at the root and then tapers distally (Evangelista et al., 2010; Freeman et al., 2013).

The location of the AB is significant for blood flow maintenance during diastole. The AB is located between the aortic root and the descending aorta, with the maximal diameter of the AB occurring near the innominate artery—an artery that carries blood to the brain (Figure 1) (King, 1977). The position of the AB coupled with a narrow descending aorta and high systemic vascular resistance during diving promotes blood flow to the brain during diving (King, 1977; Turner, 1888) as the innominate artery becomes the path of least resistance. Like other pinnipeds (e.g., Drabek, 1975), the maximum diameter of the AB occurred distal to the aortic root and proximal to the transverse arch in the northern fur seals and Steller sea lions suggesting that these species are similarly equipped for diving with low HRs.

The functional properties of the aorta are determined by their physical properties, such as vessel diameter and wall thickness (Sokolis et al., 2002). The Asc Ao diameters we measured in northern fur seals and Steller sea lions were both greater than expected for their body size based on an allometric equation for terrestrial mammals weighing 0.017–527.0 kg (Figure 3) (Holt et al., 1981). These results indicate that the entire Asc Ao is enlarged—not only the AB. The Asc Ao we measured in Steller sea lions (4.72 cm) is similar to aortic root diameters measured in bottlenose dolphins (*Tursiops truncatus*; 4.34 cm) (Chetboul et al., 2012) and southern sea lions (*Otaria flavenscens*; 4.78 cm) (Castro et al., 2018), suggesting that a large diameter aorta may be an adaptation for an aquatic lifestyle.

Larger diameter blood vessels require thicker walls to generate the same amount of inward pressure on the blood (Law of Laplace). The Ao IMT we measured in northern fur seals and Steller sea lions were comparable to those measured from histological sections of cetacean Asc Aos (0.18–1.10 cm) (Mompeó et al., 2020, 2022). Ao IMT was thinnest in northern fur seals (0.14 cm) and thickest in a sperm whale (1.10 cm; *Physeter macrocephalus*) (Mompeó et al., 2022). Steller sea lions had an intermediate thickness (0.27 cm) that closely matched the average value of three dolphin species (0.27 cm; *Delphinus delphis*, *Stenella coeruleoalba*, *Stella frontalis*) (Mompeó et al., 2020). Although histological measurements of aortic wall thickness are not exactly comparable to those measured by echocardiography, there is good agreement between the two techniques (Pandian et al., 1988; Wong et al., 1993).

Within the Delphinidae family, there is some indication that deeper diving species that usually also dive for longer durations have thicker aortic walls (Mompeó et al., 2022). However, a definitive correlation between dive depth and aortic wall thickness has yet to be established. Northern fur seals and Steller sea lions are shallow divers that routinely dive for short durations of ~2 min (Gentry et al., 1986; Gerlinsky et al., 2013; Merrick & Loughlin, 1997). It is, therefore, not surprising that they have thinner aortic walls than species such as the sperm whale that routinely dive for ~45 min (Watwood et al., 2006). However, aortic wall thickness alone does not seem to be the most important factor impacting diving in marine mammals. Comparisons of deep-diving (>500 m) whale species suggest that the decrease in aortic wall thickness that occurs along the length of the aorta, from a relatively thick Asc Ao to a thinner descending aorta, is the most critical feature (Mompeó et al., 2022). The combination of a thick-walled Asc Ao and thinner-walled descending aorta provides the ideal structure for shifting blood to the brain and heart during peripheral vasoconstriction. Unfortunately, we were unable to measure the wall thickness of the descending aorta, and, therefore, cannot assess how much its wall thickness differs from that of the AB.

In northern fur seals and Steller sea lions, the diameter of the AB is approximately the same size as the aortic root at the level of the SoV. In humans, larger aortic roots are associated with reduced afterload and larger SV (Sahlen et al., 2016), and both the aortic root and Asc Ao show a positive correlation between SV and body size (Davis et al., 2014). The similarity in size of the AB and aortic root in pinnipeds suggests that AB size is likely related to these hemodynamic factors as well.

As one function of the AB is to store and release blood, it is logical that this structure would be appropriately sized to accommodate SV. The SVs we measured in anesthetized northern fur seals and Steller sea lions were consistent with the predicted values for terrestrial mammals based on body mass (Casha et al., 2017; Mortola, 2015; Stahl, 1967) and support the results of He and colleagues (2023) who found no significant difference in SV scaling among marine and terrestrial mammals; that is, SV has not undergone evolutionary adaptation for aquatic life. However, we come to this conclusion based on a handful of previously published measurements of SV in marine mammals and from our measurements of SV obtained under anesthesia. The effect of isoflurane anesthesia on SV in otariids is unknown, but has been reported to decrease SV of terrestrial species by 14.3%–58.1% of resting values (Brett et al., 1987; Murray et al., 1992; Sousa et al., 2008). Therefore, we cannot be certain that the SVs we measured are comparable to resting values.

Despite obtaining measurements under anesthesia, we observed that the fur seals and sea lions had similar SVs to awake marine mammal species of similar size. The SVs and BWs of the adult sea lions in our study (IQR: 124.2–206.2 mL; IQR: 198.6–215.4 kg) were similar to bottlenose dolphins (104–177 mL; 143–212 kg) (Miedler et al., 2015), and those of the fur seals in our study (IQR: 25.2–46.8 mL; IQR: 30.8–35.8 kg) were similar to harbor seals (*Phoca vitulina*; 31.2–100.2 mL; 15–40 kg) (Kjekshus et al., 1982; Murdaugh et al., 1966; Ponganis et al., 1990). Interestingly, the 4-year-old Steller sea lion in our study had a lower SV (131.0 mL vs. 147.00 mL), but weighed more (139 vs. 107 kg) than an awake southern sea lion (Díaz et al., 2023). This difference may reflect our use of anesthesia or could indicate species-specific or age-related variation in SV.

It is not surprising that marine mammals do not have larger SVs than expected based on scaling arguments because consistently pumping a greater volume of blood than needed would be

energetically expensive. Rather than changes in SV, it appears that the degree of peripheral vasoconstriction regulates the volume of blood that fills the AB in proportion to what is needed during the diastolic period. In theory, increasing SV while diving could allow for lower HRs and increased vasoconstriction, which in turn could result in longer dive times, but such a change would not be without consequences. Clearly, more research is needed to determine if changes in SV during a dive contributes to diving capacity.

4.2 | AB development

The AB is present in young pinnipeds (Drabek, 1975; Drabek & Burns, 2002; King, 1977; Nie, 1985) and increases in size with growth and development (Nie, 1985), suggesting that the AB is apparent even before any cardiovascular requirements associated with diving. Regardless, there may be a training effect from repeated dives that further increases AB size. Diving capacity, in terms of maximum dive depth and duration, in northern fur seal and Steller sea lion pups increases with age (Baker & Donohue, 2000; Lea et al., 2010; Lee et al., 2014; Pitcher et al., 2005; Rehberg & Burns, 2008) and is expected to coincide with increased HR control and lower apneic HRs, as observed in harbor seal pups (Greaves et al., 2004; Lapierre et al., 2004).

The development of physiological responses to diving has the potential to affect the vasculature, much like the training effects experienced by human athletes. For example, the repeated and sustained periods of high CO that athletes experience are thought to contribute to the finding that they have larger aortic roots than nonathletes (Iskandar & Thompson, 2013; Limongelli et al., 2023), and that endurance athletes have the largest aortic roots (Limongelli et al., 2023). The athletic maneuvers and regular sustained swimming activity of pinnipeds could similarly contribute to how the AB develops, but direct measurements of CO and SV from developing individuals are needed to test this hypothesis.

It is uncertain how development and diving exercise have affected the growth of the AB in the 4-year-old sea lion we examined. Unsurprisingly, this sea lion had smaller aortic diameters than the adult sea lions in our study. These results fit the expected pattern for a younger animal of the same species and are consistent with growth and development of the Asc Ao (Drabek & Burns, 2002; Nie, 1985), and cardiovascular physiology (He et al., 2023; Hicks et al., 2004; Noren, 2020). Younger mammals also have faster HRs, which we observed in this Steller sea lion, and contributed to the larger CO observed. Despite having a larger LVOT VTI than adult sea lions, the 4-year-old still had a smaller SV due to its smaller LVOT.

4.3 | Interpreting the effects of isoflurane and atropine on hemodynamics

By necessity, measurements were taken under isoflurane anesthesia and atropine was used to experimentally alter HR, but each of these chemicals could potentially affect other aspects of hemodynamics. Isoflurane anesthesia is expected to increase HR and vasodilation by removing vagal stimulation (Haulena, 2014), opposite to what occurs during the dive response, and atropine is also expected to increase HR as it is clinically administered to counter the effects of unwanted bradycardia. As a result, our findings must be considered in the context of pharmacologically manipulated northern fur seals and Steller sea lions, and care should be taken when extrapolating to resting, swimming, and diving animals.

The northern fur seals and Steller sea lions we measured had different physiological responses from one another to atropine. HRs of the sea lions increased by 25.6%, which suggests that isoflurane anesthesia removed vagal stimulation as anticipated. In contrast, the HRs of the fur seals did not increase, indicating that the anesthetized fur seals had minimal vagal stimulation for atropine to act on. Despite the lack of statistical significance, we observed a large increase in HR in one fur seal after atropine administration. It is unclear why such a strong physiological response was noted in this individual but not others. In contrast to HR, the SVs of the fur seals and sea lions did not significantly change after atropine administration in either species. However, there was a difference in the direction of change whereby atropine tended to decrease SV in the fur seals and increase SV in the sea lions.

There are a few possible explanations for the different responses of the northern fur seals and Steller sea lions to atropine. For example, the fur seals and sea lions may have responded differently to isoflurane, or the preanesthesia masking procedure leaving them with different levels of autonomic activation. However, it is also possible that both species were similarly affected by the preanesthesia protocol and isoflurane anesthesia. If that is the case, the lack of change in HR observed in the fur seals postatropine suggests that they have lower parasympathetic activation than the sea lions while resting. Considering the vagal activity associated with diving (e.g., Ponganis et al., 2017), this could partially explain why the northern fur seals have similar routine dive times to the Steller sea lions despite having a smaller body size, which has implications for diving capability in marine mammals. In other words, our results suggest that fur seals have greater scope for increasing vagal activity than Steller sea lions and thus can achieve longer dives than expected for their body mass.

4.4 | AB dynamics

As expected, the AB of the northern fur seals and Steller sea lions expanded during systole when blood was ejected from the LV and relaxed during diastole as it pushed blood into the circulation. However, we were also able to observe how the AB mediated blood flow at different HRs. We had expected that AB diameter would be largest when HR was lowest to provide the largest reservoir of blood to maintain flow during the longer diastolic period. However, we found no statistically significant changes in AB dimensions of the northern fur seals and Steller sea lions with atropine compared to

isoflurane only and no consistency among individuals. This was despite seeing a 25.6% increase in HR in the sea lions after atropine administration. Unfortunately, the timing of our recordings which included instantaneous HR for one- to two-beats did not capture the maximum increase in HR that we observed during the entire postatropine period, perhaps impinging on our ability to detect changes in AB size in relation to HR. It appears that changes in peripheral vascular resistance need to be considered alongside changes in HR when evaluating AB dynamics in future studies. The diameter of the AB likely increases in response to increase peripheral vascular resistance, which we did not monitor. Future studies examining AB dynamics should also consider using a species with a reliably sharp decrease in HR, such as elephant seals, and record multiple beat loops to address whether the AB expands more during periods of low HR to support blood flow maintenance. Such an experiment could also be done with a species that is trained for voluntary transesophageal echocardiography, such as bottlenose dolphins Sklansky et al., 2006), that can submerge and reliably decrease their HR at the time of recording.

Despite the novel measurements we obtained, additional research is needed to examine the balance between AB size, SV, vasoconstriction, and HR in diving mammals. A clear picture has not yet emerged on how these factors interact to maintain circulation during diving in free-swimming animals. Despite using isoflurane anesthesia and atropine—which are known to affect CO—we observed that the AB supports constant blood flow in Steller sea lions with HRs ranging from 53.8 to 67.8 bpm and northern fur seals with HRs ranging from 106.0 to 128.7 bpm, and established a link between the diameter of the AB and SoV suggesting that AB size and SV are connected.

5 | CONCLUSION

This in vivo examination of the Asc Ao of northern fur seals and Steller sea lions documents the relationship between AB structure and blood flow dynamics. Highlights include exploring the relationship between AB wall thickness and dive duration, establishing a connection between AB size and SV, and verifying the change in AB size that occurs during the cardiac cycle. Overall, our findings relating AB size to SV and showing that the AB functions as expected over a narrow range of HRs support the contention that the AB is an important structure for maintaining blood flow in diving mammals.

ACKNOWLEDGMENTS

We appreciate the support provided by cardiologists Shreya Moodley and Kandice Mah from BC Children's Hospital who performed the echocardiograms, the veterinary staff and trainers at the Vancouver Aquarium, and members of UBC's Marine Mammal Research Unit who assisted with the procedures. This research was funded through a ReNewZoo grant to R. L. S. and A. W. T. and NSERC Discovery Grants to D. A. S. R. and A. W. T.

CONFLICT OF INTEREST STATEMENT

The authors declare no conflict of interest.

DATA AVAILABILITY STATEMENT

The data that support the findings of this study are available from the corresponding author upon reasonable request.

ORCID

Rhea L. Storlund http://orcid.org/0000-0001-6056-1852

REFERENCES

Baker, J. D., & Donohue, M. J. (2000). Ontogeny of swimming and diving in Northern fur seal (*Callorhinus ursinus*) pups. *Canadian Journal of Zoology*, *78*, 100–109.

Blix, A. S. (2018). Adaptations to deep and prolonged diving in phocid seals. *Journal of Experimental Biology*, *221*, 1–13.

Blix, A. S., Eisner, R., & Kjekshus, J. K. (1984). How seals avoid myocardial infarction when they should have got it. *European Surgical Research*, *16*, 22–27.

Blix, A. S., Kuttner, S., & Messelt, E. B. (2016). Ascending aorta of hooded seals with particular emphasis on its vasa vasorum. *American Journal of Physiology-Regulatory, Integrative and Comparative Physiology*, *311*, R144–R149.

Brett, C. M., Teitel, D. F., Heymann, M. A., & Rudolph, A. M. (1987). The cardiovascular effects of isofiurane in lambs. *Anesthesiology*, *67*, 60–65.

Butler, P. J. (1982). Respiratory and cardiovascular control during diving in birds and mammals. *Journal of Experimental Biology*, *100*, 195–221.

Cabanac, A. (2002). Contracted spleen in seals, estimates of dilated organs, and diving capacity. *Polar Biology*, *25*, 1–4.

Cabanac, A. J. (2000). Blood volume in hooded seals: Implications for diving capacity. *Canadian Journal of Zoology*, *78*, 1293–1299.

Campbell, K. B., Rhode, E. A., Cox, R. H., Hunter, W. C., & Noordergraaf, A. (1981). Functional consequences of expanded aortic bulb: A model study. *American Journal of Physiology-Regulatory, Integrative and Comparative Physiology*, *240*, R200–R210.

Casha, A. R., Camilleri, L., Manché, A., Gatt, R., Gauci, M., Camilleri-Podesta, M.-T., Grima, J. N., Scarci, M., & Chetcuti, S. (2017). Physiological rules for the heart, lungs and other pressure-based organs. *Journal of Thoracic Disease*, *9*, 3793–3801.

Castellini, M. A., Baskurt, O., Castellini, J. M., & Meiselman, H. J. (2010). Blood rheology in marine mammals. *Frontiers in Physiology*, *1*, 1–8.

Castro, E. F., Dassis, M., De León, M. C., Rodríguez, E., Davis, R. W., Saubidet, A., Rodríguez, D. H., & Díaz, A. (2018). Echocardiographic left ventricular structure and function in healthy, non-sedated southern sea lions (*Otaria flavescens*). *Aquatic Mammals*, *44*, 405–410.

Chetboul, V., Lichtenberger, J., Mellin, M., Mercera, B., Hoffmann, A. C., Chaix, G., Trehiou-Sechi, E., Misbach, C., Petit, A., Lefebvre, H. P., Gaide, N., Tissier, R., & Delfour, F. (2012). Within-day and between-day variability of transthoracic anatomic M-mode echocardiography in the awake bottlenose dolphin (*Tursiops truncatus*). *Journal of Veterinary Cardiology*, *14*, 511–518.

Davis, A. E., Lewandowski, A. J., Holloway, C. J., Ntusi, N. A., Banerjee, R., Nethononda, R., Pitcher, A., Francis, J. M., Myerson, S. G., Leeson, P., Donovan, T., Neubauer, S., & Rider, O. J. (2014). Observational study of regional aortic size referenced to body size: Production of a cardiovascular magnetic resonance nomogram. *Journal of Cardiovascular Magnetic Resonance*, *16*, *9*.

Dennison, S. E., Forrest, L., & Gulland, F. M. D. (2009). Normal thoracic radiographic anatomy of immature California sea lions (*Zalophus*

californianus) and immature Northern elephant seals (*Mirounga angustirostris*). *Aquatic Mammals*, *35*, 36–42.

Díaz, A., Dassis, M., De León, C., Faiella, A., Olguin, J., Saubidet, A., Rodríguez, D. H., Castro, E. F., & Diaz, A. (2023). Doppler echocardiography in a healthy, non-sedated southern sea lion (*Otaria flavescens*) - a preliminary approach about the feasibility and clinical utility. *Veterinary Research Communications*, *47*, 953–961.

Drabek, C. M. (1975). Some anatomical aspects of the cardiovascular system of Antarctic seals and their possible functional significance in diving. *Journal of Morphology*, *145*, 85–105.

Drabek, C. M., & Burns, J. M. (2002). Heart and aorta morphology of the deep-diving hooded seal (*Cystophora cristata*). *Canadian Journal of Zoology*, *80*, 2030–2036.

Elsner, R., Franklin, D. L., Van Citters, R. L., & Kenney, D. W. (1966). Cardiovascular defense against asphyxia. *Science*, *153*, 941–949.

Evangelista, A., Flachskampf, F. A., Erbel, R., Antonini-Canterin, F., Vlachopoulos, C., Rocchi, G., Sicari, R., Nihoyannopoulos, P., Zamorano, J., Pepi, M., Breithardt, O. A., & Plonska-Gosciniak, E. (2010). Echocardiography in aortic diseases: EAE recommendations for clinical practice. *European Journal of Echocardiography*, *11*, 645–658.

Fox, J., & Weisberg, S. (2019). *An {R} companion to applied regression*. Sage. https://socialsciences.mcmaster.ca/jfox/Books/Companion/

Freeman, L. A., Young, P. M., Foley, T. A., Williamson, E. E., Bruce, C. J., & Greason, K. L. (2013). CT and MRI assessment of the aortic root and ascending aorta. *American Journal of Roentgenology*, *200*, W581–W592.

Gentry, R. L., Kooyman, G. L., & Goebel, M. E. (1986). Feeding and diving behavior of northern fur seals In R. L. Gentry & G. L. Kooyman (Eds.), *Fur seals: Maternal strategies on land and at sea* (pp. 61–78). Princeton University Press.

Gerlinsky, C. D., Rosen, D. A. S., & Trites, A. W. (2013). High diving metabolism results in a short aerobic dive limit for Steller sea lions (*Eumetopias jubatus*). *Journal of Comparative Physiology B*, *183*, 699–708.

Greaves, D. K., Hughson, R. L., Topor, Z., Schreer, J. F., Burns, J. M., & Hammill, M. O. (2004). Changes in heart rate variability during diving in young harbor seals, *Phoca vitulina*. *Marine Mammal Science*, *20*, 861–871.

Guimarães, J. P., Mari, R. B., Le Bas, A., & Watanabe, I. S. (2014). Adaptive morphology of the heart of southern-fur-seal (*Arctocephalus australis* – Zimmermamm, 1783). *Acta Zoologica*, *95*, 239–247.

Haulena, M. (2014). Otariid seals. In G. West, D. Heard, & N. Caulket (Eds.), *Zoo animal and wildlife immobilization and anesthesia* (2nd ed., pp. 661–672). John Wiley & Sons, Inc.

He, R. S., De Ruiter, S., Westover, T., Somarelli, J. A., Blawas, A. M., Dayanidhi, D. L., Singh, A., Steves, B., Driesinga, S., Halsey, L. G., & Fahlman, A. (2023). Allometric scaling of metabolic rate and cardiorespiratory variables in aquatic and terrestrial mammals. *Physiological Reports*, *11*, 1–11.

Hicks, J. L., O'Hara Hines, R. J., Schreer, J. F., & Hammill, M. O. (2004). Correlation of depth and heart rate in harbour seal pups. *Canadian Journal of Zoology*, *82*, 1147–1156.

Holt, J. P., Rhode, E. A., Holt, W. W., & Kines, H. (1981). Geometric similarity of aorta, venae cavae, and certain of their branches in mammals. *American Journal of Physiology-Regulatory, Integrative and Comparative Physiology*, *241*, R100–R104.

Iskandar, A., & Thompson, P. D. (2013). A meta-analysis of aortic root size in elite athletes. *Circulation*, *127*, 791–798.

Kassambara, A. 2023. rstatix: Pipe-friendly framework for basic statistical tests. https://rpkgs.datanovia.com/rstatix/

King, J. E. (1977). Comparative anatomy of the major blood vessels of the sealions *Neophoca* and *Phocarctos*; with comments on the differences between the otariid and phocid vascular systems. *Journal of Zoology*, *181*, 69–94.

Kjekshus, J. K., Blix, A. S., Elsner, R., Hol, R., & Amundsen, E. (1982). Myocardial blood flow and metabolism in the diving seal. *American Journal of Physiology-Regulatory, Integrative and Comparative Physiology*, *242*, R97–R104.

Kooyman, G. L., & Ponganis, P. J. (1998). The physiological basis of diving to depth: birds and mammals. *Annual Review of Physiology*, *60*, 19–32.

Lapierre, J. L., Schreer, J. F., Burns, J. M., & Hammill, M. O. (2004). Developmental changes in cardiorespiratory patterns associated with terrestrial apnoeas in harbour seal pups. *Journal of Experimental Biology*, *207*, 3891–3898.

Lea, M., Johnson, D., Melin, S., Ream, R., & Gelatt, T. (2010). Diving ontogeny and lunar responses in a highly migratory mammal, the northern fur seal *Callorhinus ursinus*. *Marine Ecology Progress Series*, *419*, 233–247.

Lee, O., Andrews, R. D., Burkanov, V. N., & Davis, R. W. (2014). Ontogeny of early diving and foraging behavior of northern fur seal (*Callorhinus ursinus*) pups from Bering Island, Russia. *Marine Biology*, *161*, 1165–1178.

Limongelli, G., Monda, E., Lioncino, M., Di Paolo, F., Ferrara, F., Vriz, O., Calabro, P., Bossone, E., & Pelliccia, A. (2023). Aortic root diameter in highly-trained competitive athletes: Reference values according to sport and prevalence of aortic enlargement. *Canadian Journal of Cardiology*, *39*, 889–897.

Merrick, R. L., & Loughlin, T. R. (1997). Foraging behavior of adult female and young-of-the-year Steller sea lions in Alaskan waters. *Canadian Journal of Zoology*, *75*, 776–786.

Miedler, S., Fahlman, A., Valls Torres, M., Alvaro Alvarez, T., & Garcia-Parraga, D. (2015). Evaluating cardiac physiology through echocardiography in bottlenose dolphins: Using stroke volume and cardiac output to estimate systolic left ventricular function during rest and following exercise. *Journal of Experimental Biology*, *218*, 3604–3610.

Mompeó, B., Pérez, L., Fernández, A., Saavedra, P., Rivero, M., Arbelo, M., Arregui, M., Suárez-Santana, C., & Bernaldo-de-Quiros, Y. (2020). Morphological structure of the aortic wall in three Delphinid species with shallow or intermediate diving habits: Evidence for diving adaptation. *Journal of Morphology*, *281*, 377–387.

Mompeó, B., Sacchini, S., Quintana, M. P., Rivero, M., Consoli, F., Fernández, A., & Bernaldo de Quirós, Y. (2022). Morphological structure of the aortic wall in deep diving cetacean species: Evidence for diving adaptation. *Veterinary Sciences*, *9*, 424.

Mortola, J. P. (2015). The heart rate—Breathing rate relationship in aquatic mammals: A comparative analysis with terrestrial species. *Current Zoology*, *61*, 569–577.

Murdaugh HV, H., Robin, E., Millen, J., Drewry, W., & Weiss, E. (1966). Adaptations to diving in the harbor seal: Cardiac output during diving. *American Journal of Physiology-Legacy Content*, *210*, 176–180.

Murie, D. J. (1874). Researches upon the anatomy of the Pinnipedia.—(Part III.) Descriptive anatomy of the sea-lion (*Otaria jubata*). *The Transactions of the Zoological Society of London*, *8*, 501–582.

Murray, D. J., Forbes, R. B., & Mahoney, L. T. (1992). Comparative hernodynamic depression of halothane versus isoflurane in neonates and infants: An echocardiographic study. *Anesthesia and Analgesia*, *74*, 329–337.

Nichols, W. W., O'Rourke, M. F., & Vlachopoulos, C. (2011). McDonald's blood flow in arteries W. W. Nichols, M. F. O'Rourke, & C. Vlachopoulos (Eds.), *Theoretical, experimental and clinical principles* (6th ed.). Taylor & Francis Group, LLC.

Nie, C. J. van (1985). The bulbus aortae (*aorta ascendens*) in the growing common seal (*Phoca vitulina vitulina*) (a morphological approach). *Aquat Mamm*, *11.3*, 71–74.

Noren, S. R. (2020). Postnatal development of diving physiology: Implications of anthropogenic disturbance for immature marine mammals. *Journal of Experimental Biology*, *223*, 1–11.

Pandian, N. G., Kreis, A., Brockway, B., Isner, J. M., Sacharoff, A., Boleza, E., Caro, R., & Muller, D. (1988). Ultrasound angioscopy: Real-time, two-dimensional, intraluminal ultrasound imaging of blood vessels. *The American Journal of Cardiology*, *62*, 493–494.

Pitcher, K. W., Rehberg, M. J., Pendleton, G. W., Raum-Suryan, K. L., Gelatt, T. S., Swain, U. G., & Sigler, M. F. (2005). Ontogeny of dive performance in pup and juvenile Steller sea lions in Alaska. *Canadian Journal of Zoology*, *83*, 1214–1231.

Ponganis, P., Kooyman, G., Zornow, M., Castellini, M., & Croll, D. (1990). Cardiac output and stroke volume in swimming harbor seals. *Journal of Comparative Physiology B*, *160*, 473–482.

Ponganis, P. J. (2015). Adaptations in cardiovascular anatomy and hemodynamics, *Diving physiology of marine mammals and seabirds*. Cambridge University Press.

Ponganis, P. J., McDonald, B. I., Tift, M. S., & Williams, C. L. (2017). Heart rate regulation in diving sea lions: The vagus nerve rules. *Journal of Experimental Biology*, *220*, 1372–1381.

Qvist, J., Hill, R. D., Schneider, R. C., Falke, K. J., Liggins, G. C., Guppy, M., Elliot, R. L., Hochachka, P. W., & Zapol, W. M. (1986). Hemoglobin concentrations and blood gas tensions of free-diving Weddell seals. *Journal of Applied Physiology*, *61*, 1560–1569.

R Core Team. 2022. R: A language and environment for statistical computing.

Rehberg, M. J., & Burns, J. M. (2008). Differences in diving and swimming behavior of pup and juvenile Steller sea lions (*Eumetopias jubatus*) in Alaska. *Canadian Journal of Zoology*, *86*, 539–553.

Rhode, E. A., Elsner, R., Peterson, T. M., Campbell, K. B., & Spangler, W. (1986). Pressure-volume characteristics of aortas of harbor and Weddell seals. *American Journal of Physiology-Regulatory, Integrative and Comparative Physiology*, *251*, R174–R180.

RStudio Team. (2022). RStudio: Integrated development environment for R. http://www.rstudio.com/

Sahlén, A., Hamid, N., Amanullah, M. R., Fam, J. M., Yeo, K. K., Lau, Y. H., Lam, C. S. P., & Ding, Z. P. (2016). Impact of aortic root size on left ventricular afterload and stroke volume. *European Journal of Applied Physiology*, *116*, 1355–1365.

Schindelin, J., Arganda-Carreras, I., Frise, E., Kaynig, V., Longair, M., Pietzsch, T., Preibisch, S., Rueden, C., Saalfeld, S., Schmid, B., Tinevez, J.-Y., White, D. J., Hartenstein, V., Eliceiri, K., Tomancak, P., & Cardona, A. (2012). Fiji: An open-source platform for biological-image analysis. *Nature Methods*, *9*, 676–682.

Shadwick, R. E., & Gosline, J. M. (1994). Arterial mechanics in the fin whale suggest a unique hemodynamic design. *American Journal of Physiology-Regulatory, Integrative and Comparative Physiology*, *267*, R805–R818.

Shadwick, R. E., & Gosline, J. M. (1995). Arterial windkessels in marine mammals. *Symposia of the Society for Experimental Biology*, *49*, 243–252.

Sklansky, M., Levine, G., Havlis, D., West, N., Renner, M., Rimmerman, C., & Stone, R. (2006). Echocardiographic evaluation of the bottlenose dolphin (*Tursiops truncatus*). *Journal of Zoo and Wildlife Medicine: Official Publication of the American Association of Zoo Veterinarians*, *37*, 454–463.

Sokolis, D. P., Boudoulas, H., Kavantzas, N. G., Kostomitsopoulos, N., Agapitos, E. V., & Karayannacos, P. E. (2002). A morphometric study of the structural characteristics of the aorta in pigs using an image analysis method. *Anatomia, Histologia, Embryologia*, *31*, 21–30.

Sousa, M. G., Carareto, R., De-Nardi, A. B., Brito, F. L., Nunes, N., & Camacho, A. A. (2008). Effects of isoflurane on echocardiographic parameters in healthy dogs. *Veterinary Anaesthesia and Analgesia*, *35*, 185–190.

Stahl, W. R. (1967). Scaling of respiratory variables in mammals. *Journal of Applied Physiology*, *22*, 453–460.

Stephenson, R. (2005). Physiological control of diving behaviour in the Weddell seal *Leptonychotes weddelli*: A model based on cardiorespiratory control theory. *Journal of Experimental Biology*, *208*, 1971–1991.

Storlund, R. L., Rosen, D. A. S., Margiocco, M., Haulena, M., & Trites, A. W. (2021). Cardiac examinations of anesthetized Steller sea lions (*Eumetopias jubatus*), northern fur seals (*Callorhinus ursinus*), and a walrus (*Odobenus rosmarus*). *Journal of Zoo and Wildlife Medicine*, *52*, 507–519.

Thornton, S. J., Hochachka, P. W., Crocker, D. E., Costa, D. P., LeBoeuf, B. J., Spielman, D. M., & Pelc, N. J. (2005). Stroke volume and cardiac output in juvenile elephant seals during forced dives. *Journal of Experimental Biology*, *208*, 3637–3643.

Turner, W. (1888). Viscera of elephant seal. *Report on the Scientific Results of the Voyage of H.M.S. Challenger*, *26*, 135–138.

Watwood, S. L., Miller, P. J. O., Johnson, M., Madsen, P. T., & Tyack, P. L. (2006). Deep-diving foraging behaviour of sperm whales (*Physeter macrocephalus*). *Journal of Animal Ecology*, *75*, 814–825.

Wong, M., Edelstein, J., Wollman, J., & Bond, M. G. (1993). Ultrasonic-pathological comparison of the human arterial wall. Verification of intima-media thickness. *Arteriosclerosis and Thrombosis: A Journal of Vascular Biology*, *13*, 482–486.

Zapol, W. M., Liggins, G. C., Schneider, R. C., Qvist, J., Snider, M. T., Creasy, R. K., & Hochachka, P. W. (1979). Regional blood flow during simulated diving in the conscious Weddell seal. *Journal of Applied Physiology*, *47*, 968–973.

SUPPORTING INFORMATION

Additional supporting information can be found online in the Supporting Information section at the end of this article.

How to cite this article: Storlund, R. L., Rosen, D. A. S., Haulena, M., Sanatani, S., Vander Zaag, J., & Trites, A. W. (2024). Ultrasound images of the ascending aorta of anesthetized northern fur seals and Steller sea lions confirm that the aortic bulb maintains continuous blood flow. *Journal of Experimental Zoology Part A: Ecological and Integrative Physiology*, 1–12. https://doi.org/10.1002/jez.2799